NASA Technical Memorandum 87799

A Method of Calculating the Total Flow From a Given Sea Surface Topography

Desiraju B. Rao, Stephen D. Steenrod,
and Braulio V. Sanchez

APRIL 1987

NASA

NASA Technical Memorandum 87799

A Method of Calculating the Total Flow From a Given Sea Surface Topography

Desiraju B. Rao
National Meteorological Center
Washington, D.C.

Stephen D. Steenrod
Applied Research Corporation
Landover, Maryland

Braulio V. Sanchez
Goddard Space Flight Center
Greenbelt, Maryland

National Aeronautics
and Space Administration

Scientific and Technical
Information Branch

1987

TABLE OF CONTENTS

A Method of Calculating the Total Flow From a Given Sea Surface Topography

Desiraju B. Rao, Stephen D. Steenrod, and Braulio V. Sanchez

INTRODUCTION

Altimetric measurements from a satellite yield the sea surface topography on a global basis. Such a sea surface topography represents the sum of (i) the marine geoid, which is the shape the ocean surface assumes when at rest, (ii) the departure of the ocean surface from the geoid due to the near surface ocean circulations, and (iii) a variety of errors related to the determination of satellite orbit, tides, etc. See Wunsch and Gaposchkin (1980) and report of the TOPEX Science Working Group (1981) for a review of the errors associated with satellite altimetric measurements. If the errors due to source (iii) are eliminated and if one knows the shape of the geoid, in principle, we have the residual sea surface topography associated with dynamics of the ocean circulation. Since the surface elevation is a simple scalar variable and reflects oceanic processes occurring at depth, satellite altimetry offers the potential to study global ocean circulation if it can be measured with the necessary accuracy – particularly when treated together with other available hydrographic data. See, for example, the analysis of the Seasat altimetric residuals by Tai and Wunsch (1983) and Tai (1983).

The primary advantage of being able to measure the sea surface topography is the fact that one can directly compute the surface pressure gradients and the associated geostrophic currents. These currents would then be the reference velocities for the integration of the observed density field via the ''thermal wind'' equation to provide absolute currents at depth. Hence the altimetric measurements of the sea surface eliminate the necessity of invoking the existence of an arbitrary level of no motion which can only provide the relative currents. However, if certain assumptions are invoked and a conceptual model of ocean circulation dynamics is adapted, it is possible to infer more than the ''near surface geostrophic currents'' from the measured sea surface topography. Admittedly the ocean circulation is a complex result of forcing by the wind stresses and the atmospheric heating and cooling. The circulation consists of both barotropic and baroclinic components and exhibits spatial and temporal variabilities on a wide range of scales. Nevertheless, in this preliminary attempt, a working assumption is made that the circulation dynamics in the upper layers of the ocean are dominated by wind driven forcing much like in the Stommel (1948) study. When the upper layer of an ocean is spun up to a steady state under the influence of a wind stress and a linear bottom friction, the circulation dynamics represent a balance between the Coriolis, pressure gradient, wind stress, and bottom friction forces. Hence the observed surface topography represents a more complicated balance of forces than just geostrophy even in this simple conceptual dynamical framework.

We present a method here that, given a data field of sea surface topography, allows the recovery through an objective analysis procedure of the total flow field, which may be viewed as the sum of a geostrophic and an ageostrophic component if one so desires. However, since geostrophic considerations become progressively weak as one approaches the equator and the flows become more and more ageostrophic, we will simply refer to the flow derived from our calculations as the actual or total flow. Since no geostrophic considerations are imposed in the analytical development, the analysis procedure outlined here is not affected by the vanishing of the Coriolis parameter at the equator in calculating the currents from the surface pressure field.

The results presented deal with the steady circulation in an ideal rectangular basin on a beta plane. The theory is, however, also valid to study the transient circulation so long as the circulation is assumed to be non-divergent.

The theory is based on developing a spectrum of characteristic functions for the stream function field and the surface height field. Given a wind field these functions are then used to represent the forced solution for the velocity and surface pressure fields in which the expansion coefficients for both fields are required to be the same. Such a calculation serves a two-fold purpose. The first one is that the forced solution indicates which of the spectral components are most energetic so that these may be used in the objective analysis of the height field data. The second purpose is that when an objective analysis is performed on a limited set of surface height field data points extracted from the theoretical solution, this solution would serve the function of the ''true'' solution to validate the objective analysis procedure. The reason for using a limited

set of available data in dealing with real altimetric signals is simply due to the errors in our knowledge of the geoid over various parts of the global ocean and the consequent contamination of the altimetric retrievals over these regions of the global ocean. Elimination of data in regions of serious uncertainty in the altimetric retrievals and the use of functions characteristic of a given basin should result in extracting the oceanographic signal from the measurements in a most optimal way. In the objective analysis the most energetic functions, as indicated by the theoretical solution, would be used and the coefficients of expansion would be determined by linear least squares procedure. Once the expansion coefficients are thus obtained, the stream function associated with the total flow can be synthesized using the stream function characteristic modes. An additional advantage of the proposed technique is that the analytical basis of the theory allows inferences to be made on the direction of the rotational part of the wind stress. At least in the simple case presented here, the direction of the wind stress is unambiguously determined. The entire methodology described here is easily treated numerically and can be extended to deal with real world basins as will be discussed later.

THEORETICAL BASIS

In solving the problem of wind driven ocean circulation in an enclosed basin using "spectral" expansion procedures,it is possible to consider the full gravitational and rotational modes of the basin as the relevant functions. The powerful expansion technique of Eckart may then be invoked to solve the inhomogeneous problem as, for example, done by Reid (1958) and Rao (1974). Although the determination of gravitational normal modes of a closed basin is not an easy matter even for simple shapes, it is nevertheless feasible (Rao 1966). Moreover, even for natural basins numerical methods have now been developed to compute the gravitational modes reasonably accurately (Platzman 1975, 1977, Rao and Schwab 1976). Rotational modes, however, are very complex even in simple basins and for real basins they are extremely sensitive to the resolution of the shape of the basins and the bottom topographic variations as found in the above mentioned studies of Platzman, and Rao and Schwab. Since the large scale ocean circulation is primarily dominated by rotational modes and the determination process of these modes is not a "robust" one, it is felt that it would be best to avoid a representation of the solution in terms of normal modes. Instead, the solutions are developed in terms of a set of characteristic functions that are more easily determinable and are less sensitive to the resolution of the basin geometry and bottom topography. Further, this procedure avoids the dynamic "prejudice" such as absence of friction, sensitivity to spatial resolutions, etc., implicit in the actual normal modes. Indeed this is the procedure adapted by Rao and Schwab (1981) in the analysis of lake circulations and by Sanchez, Rao, and Wolfson (1985) in the analysis of tides in a lake.

The analysis presented below depends primarily on the basic assumptions that the ocean circulation is non-divergent and that the wind stress acting on it is also non-divergent. For large scale ocean circulation these assumptions can be justified using the conventional scale considerations. An additional assumption introduced is that the normal component of the wind stress is zero on the north-south boundaries for reasons to be explained later. In this study we consider a linear wind driven ocean circulation model with a linear bottom friction. The analysis can, however, be extended to take into account nonlinear dynamics if necessary. The governing equations are:

$$\frac{\partial u}{\partial t} - fv = -g\frac{\partial \zeta}{\partial x} + \frac{\tau_x}{\varrho H} - \lambda u$$

$$\frac{\partial v}{\partial t} + fu = -g\frac{\partial \zeta}{\partial y} + \frac{\tau_y}{\varrho H} - \lambda v \qquad (2.1)$$

$$\frac{\partial u}{\partial x} + \frac{\partial v}{\partial y} = 0 \qquad (2.2)$$

In the above equations, u and v are the horizontal velocities in the X (east-west) and Y (north-south) directions. f is the Coriolis parameter $= f_o + \beta y$. ζ represents the surface height fluctuation (namely, the altimetric residual of the sea surface), g the gravitational acceleration, τ_x, τ_y the wind stress, and λ the linear friction coefficient. ϱ is the water density which is taken to be $=1$ cgs and omitted from here on. The depth H in equation (2.1) is the so called depth of wind driven circulation. This depth will be taken as a constant even though such a restriction is not necessary for the analysis. If it is considered that the wind driven circulation is felt through the entire depth of the ocean and the depth H is a variable, the analysis can easily accommodate this following the line of Rao and Schwab's (1981) study.

In view of the fact that H is a constant and the flow is non-divergent, the velocity field can be expressed in terms of a stream function:

$$u = -\frac{\partial \psi}{\partial y}, \quad v = \frac{\partial \psi}{\partial x} \qquad (2.3)$$

Forming the vorticity equation from (2.1), we obtain

$$\left(\frac{\partial}{\partial t} + \lambda\right)\eta + \beta v = \frac{1}{H}\left(\frac{\partial \tau_y}{\partial x} - \frac{\partial \tau_x}{\partial y}\right) \qquad (2.4)$$

where the vertical component of vorticity η is given by

$$\eta = \nabla^2 \psi \qquad (2.5)$$

If the divergence operator is applied to equation (2.1) the result, in view of equation (2.2) and the assumption that the large scale wind stress is also non-divergent, is:

$$\nabla \cdot f\,\nabla\psi = g\nabla^2\zeta \qquad (2.6)$$

The above equation is easily recognized as the "linear balance equation" extensively used by the meteorological community in numerical weather prediction.

Even though equation (2.6) appears to be a direct consequence of the geostrophic relations

$$f\,\nabla\psi = g\nabla\zeta,$$

it should be noted that exact geostrophy is not permitted for two dimensional nondivergent flows on a rotating earth with a variable Coriolis parameter. This can be seen by taking the curl of the above relations which leads to the result that

$$\frac{\partial f}{\partial y}\frac{\partial \psi}{\partial x} = 0$$

Since $\partial f/\partial y \neq 0$, then $v = \partial\psi/\partial x$ must be $= 0$. The continuity equation then reduces to $\partial u/\partial x = 0$. Hence u itself

is zero since it has to vanish on the eastern and western boundaries of the basin leading to the conclusion that non-divergent geostrophic flow is not permitted on a beta-plane or a spherical earth. On the other hand if the bottom topography varies as a function of space, the non-divergent form of the continuity equation involves the vertically integrated transport so that

$$u = -\frac{1}{H}\frac{\partial \psi}{\partial y}, \quad v = \frac{1}{H}\frac{\partial \psi}{\partial x}$$

In this case the geostrophic statement is expressed by

$$\frac{f}{H}\nabla\psi = g\nabla\zeta$$

where ψ is now the transport stream function. Taking a curl of this yields the condition that $\nabla\frac{f}{H} \times \nabla\psi = 0$, which shows that the transport is parallel to the contours of $\frac{f}{H}$ = constant. In either case of H = constant or a variable it is clear that the stream lines and hence the flow will not be parallel to the contours of sea surface topography on a rotating earth with variable Coriolis parameter. Hence the hypothesis that, given a surface topography, one can deduce the magnitude and the direction of the near surface geostrophic current is not precisely valid over the global oceans in general and more particularly so in the low latitudes.

In the context of altimetry, if the sea surface topography is given over a domain, equation (2.6) may be viewed as an inhomogeneous elliptic equation for the stream function ψ. Since the ocean basin is considered to be closed, the boundary condition on the stream function is simply

$$\psi = 0 \text{ on the boundary.} \tag{2.7}$$

Equation (2.6) may then be solved in a straight forward manner for the stream function. Note that the stream function involved here is not just the geostrophic stream function but is associated with the full dynamics of equation (2.1). However, as mentioned earlier, the altimetric measurements over an ocean basin suffer from contamination due to various sources of error, the geoid being the main contributor. Hence it is not advisable to make an attempt to solve equation (2.6) directly without subjecting the altimetric residuals to a selective elimination of bad data points, and smoothing and extrapolating the remainder to define the surface topography at all grid points in the basin. This requires the adoption of some specific procedure. The most suitable one will be a method using some functions explicitly reflecting the properties of the basin under consideration. However, at this stage it is not obvious how to construct these functions.

In the following a procedure is described that would first establish a set of appropriate characteristic functions for the stream function. Then from these stream function modes, a separate set of characteristic functions are derived that would be relevant to the analysis of surface topography. If the vorticity field $\eta(x,y)$ is assumed to be known, equation (2.5) represents an inhomogeneous equation for ψ. With the boundary condition (2.7), conceptually the problem can again be solved to obtain the stream function. In principle it is, of course, not possible to get a field of vorticity from measurements and particularly not from altimetric retrievals. A convenient way to look at the problem is simply to consider expanding the stream function in terms of the characteristic functions of the operator ∇^2; that is, in terms of the solution to the problem:

$$\begin{aligned} \nabla^2\psi_\alpha &= -\mu_\alpha \psi_\alpha \\ \psi_\alpha &= 0 \text{ on the boundary.} \end{aligned} \tag{2.8}$$

μ_α's are the characteristic values associated with the vectors ψ_α. It is clear that (2.8) is a self-adjoint problem and the ψ_α's form an orthogonal set. The scalar index α is a proxy to an ordering of the ψ_α's in some as yet unspecified manner. Since the ψ_α's constitute a complete set, they are capable of representing any arbitrary field over the basin. Hence we can express

$$\psi = \sum_\alpha P_\alpha \psi_\alpha \tag{2.10}$$

Let the orthogonality of the ψ_α's be defined by

$$\mu_\alpha \int \psi_\alpha \psi_\beta \, dA. = \delta_{\alpha\beta}, \tag{2.11}$$

where $\delta_{\alpha\beta}$ is the Kronecker delta. The integration is performed over the area of the basin. The expansion coefficients are then given by

$$P_\alpha = \mu_\alpha \int \psi \psi_\alpha \, dA. \tag{2.12}$$

When the sum on the right hand side of equation (2.10) spans the complete spectrum of the elliptic operator in (2.8), equation (2.10) represents a least squares approximation to ψ with the usual restrictions on quadratic integrability and continuity of ψ and its derivatives. The stream function in (2.10) when it is substituted into the governing dynamical equations, determines the velocity field generated by the surface wind stress in the ocean basin under consideration. Convergence of the series (2.10) is determined by the expansion coefficients P_α, whose value is governed by the properties of the imposed wind field. The kinetic energy of the circulation in the basin is given by

$$KE = \tfrac{1}{2} \int H(u^2 + v^2) \, dA = \tfrac{1}{2} \sum_\alpha H P_\alpha^2.$$

Hence the contribution from each of the "modes" to the variance of the circulation is governed by the wind forcing

and presumably the identity of the dominant modes would change with different wind fields. Consequently, in carrying out the objective analysis, it will be useful to have an a priori idea of the dominant modes, say for example, as a function of the seasonal fields. Note that the shape of the basin influences the properties of the stream function modes through equation (2.8). If real topography is also taken into account that would influence the shapes of the modes through a variant of (2.8) as considered in Rao and Schwab (1981).

Substitute the expansion (2.10) into the vorticity equation (2.4) and use the orthogonality condition (2.11). The result is:

$$\frac{d\vec{P}}{dt} + (\lambda\, II - \underline{C})\,\vec{P} = \vec{F}, \qquad (2.13),$$

where we have defined the column vectors $\vec{P}$ and $\vec{F}$

$$\vec{P} \equiv \text{Column } (P_\alpha) \qquad (2.14)$$

$$\vec{F} \equiv \text{Column } (F_\alpha) = -\frac{1}{H}\int\left(\frac{\partial \tau_y}{\partial x} - \frac{\partial \tau_x}{\partial y}\right)\psi_\alpha \, dA.$$

In (2.13), II is the identity matrix and the elements the matrix $\underline{C}$ are defined by

$$\underline{C} \equiv (C_{\gamma\alpha}) = \beta\int \psi_\gamma \frac{\partial \psi_\alpha}{\partial x}\, dA. \qquad (2.15)$$

Hence, if the wind stress is prescribed, equation (2.13) can be solved directly for the expansion coefficients P_α and the stream function and the velocity fields can be obtained through (2.10, 2.3). If in particular, the wind stress is steady and only the steady state solution is sought, it is simply given by

$$\vec{P} = (\lambda\, II - \underline{C})^{-1}\,\vec{F} \qquad (2.16)$$

Having obtained ψ and the flow field, it remains to establish a basis to compute the associated height field solution. This is accomplished through the use of the divergence equation (2.6) which may be viewed now as an inhomogeneous equation for ζ. A convenient way to develop the height field solution is to express it in terms of the following expansion:

$$\zeta = \sum_\alpha P_\alpha\, \zeta_\alpha \qquad (2.17)$$

ζ_α's are characteristic functions for the height field. Note that in the above representation for the ζ field the expansion coefficients are deliberately chosen to be the same as those for the stream function given in (2.10). In view of the fact that the expansion coefficients in (2.10 and 17) are the same substituting the above in (2.6) one obtains

$$g\nabla^2\zeta_\alpha = \nabla \cdot f\nabla\psi_\alpha \qquad (2.18)$$

which is simply a balance equa on establishing a relation between the characteristic modes f the height field and those of the stream function field. The o perators involved on both sides of the equation are elliptic. The important aspect to note is that the zonal dependence o f the operators is the same on both sides of the equation but t he latitudinal dependence differs because of the variation of the Coriolis parameter in that direction. In view of this the boundary conditions for ζ_α are:

$$\zeta_\alpha = 0 \text{ on meridiona l boundaries} \qquad (2.19a)$$

$$g\frac{\partial \zeta_\alpha}{\partial y} = f\frac{\partial \psi_\alpha}{\partial y} \text{ on zo nal boundaries} \qquad (2.19b)$$

The second condition follows from the second momentum equation of (2.1) using the assu mption of zero wind stress normal to the zonal boundaries. Th is assumption permits the determination of basis functions fo r the height field once for all for any given basin just like th e stream function modes. Since the primary wind stress fo rce for global oceans is predominantly zonal, the assumpti on of zero meridional wind stress on the north-south bound aries is certainly a very reasonable one. Equation (2.18) subject to the conditions (2.19) can be solved by numerica l methods for any natural basin. The ζ_α's substituted into eq uation (2.17) give the surface height field associated with th e wind driven circulation.

In the above process a set of c haracteristic functions for the height field have been establi shed that would be useful for objective analysis of altimetric residuals as will be shown later. In addition, since the expan sion coefficients for both the height and flow fields are the same, once the P_α's are calculated through objective analy sis of the altimetric measurements, the stream function fie ld associated with the dynamics of equation (2.1) is also o btained. As is evident the flow field associated with these dynamics is the total flow field and not just the geostrophic component corresponding to the surface topography.

OBJECTIVE ANALYSIS

Suppose that altimetric residuals describing the sea surface topography are available at certain discrete number of points over a given basin. In view of the uncertainties involved in these data due to the sources of error mentioned earlier, some of the data would get rejected selectively. Acceptable data points obtained from this process would generally not be given over a regularly spaced grid. The resulting sea surface height field, as shown in equation (2.17), can be represented spectrally by:

$$\zeta = \sum_{\alpha=1}^{N} P_\alpha\, \zeta_\alpha \qquad (3.1)$$

The series is truncated at N modes and the N coefficients P_α are the unknowns that need to be determined from the data. If the data are available at M number of points and each point is designated as

$$\zeta_j = \zeta(x_j,y_j);\ j = 1, 2 \ldots M,$$

then equation (3.1) becomes

$$\zeta_j = \sum_{\alpha=1}^{N} P_\alpha\, \zeta_\alpha\,(x_j,\, y_j). \tag{3.2}$$

Equation (3.2) represents M number of equations in N unknowns. If M = N, a set of N equations in as many unknowns are obtained. The expansion coefficients thus determined would exactly fit the data at the observation points leading to a zero rms error at the data points. In general, however, it is preferable to take N < M so that there are fewer unknowns than equations (an overdetermined system) and determine the coefficients in a least squares sense. That is, since equation (3.2) can not be satisfied exactly, we try to minimize the rms difference which is defined by

$$E = \left[\frac{1}{M}\sum_{j=1}^{M}\left(\zeta_j - \sum_{\alpha=1}^{N} P_\alpha \zeta_{j\alpha}\right)^2\right]^{1/2} \tag{3.3}$$

where ζ_j are the height field data from altimetric measurements. If a column vector of length M × 1 is defined as

$$\vec{\zeta} \equiv \text{Column}\ (\zeta_1,\ \zeta_2,\ \ldots .\ \zeta_M)$$

then equation (3.2) can be expressed in a matrix form

$$\vec{\zeta} = \underline{B}\ \vec{P} \tag{3.4}$$

where $\underline{B}$ is a rectangular matrix of dimensions M×N with elements given by

$$\underline{B} \equiv (B_{j\alpha}) = \zeta_\alpha\,(x_j,\, y_j)$$

and $\vec{P}$ is a column vector of length N × 1 given by

$$\vec{P} \equiv \text{Column}\ (P_1,\ P_2,\ \ldots .\ P_N)$$

The elements of the matrix $\underline{B} = (B_{j\alpha})$ are the values of the characteristic modes ζ_α at the locations j and are available from the height field characteristic functions previously determined. The least squares solution to equation (3.4) is then given by

$$\vec{P} = (\underline{B}^T\, \underline{B})^{-1}\, \underline{B}^T\, \vec{\zeta} \tag{3.5}$$

where $\underline{B}^T$ is the transposed matrix. Having determined $\vec{P}$, since the functions ζ_α are known over the whole domain of the basin, the objectively analyzed sea surface topography can be mapped over the entire basin from equation (3.1). As mentioned earlier, the basis functions reflect the geometric peculiarties of an individual basin or global oceans and hence would constitute a more suitable set of functions for analyzing data than any analytical functions. Also since the basis functions used in the objective analysis of the height field are derived from the solution of the inhomogeneous problem (2.17, 18, 19), the expansion coefficients P_α can now be used to synthesize the stream function field over the basin through equation (2.10). Hence the height field analysis technique developed here permits the possibility of computing not just the geostrophic flow associated with the measured topography but the actual (or total) flow associated with the topography, Coriolis forces, surface wind stress, and bottom friction. Another aspect of the technique to notice is that the characteristic modes of the stream function and the height field are *completely independent* of the values assigned to the depth H of the wind driven ocean or the friction coefficient in the momentum equations (2.1). Consequently these parameters, which are by no means well established constants, have no influence on the analysis of the surface topography and the synthesis of the stream function field.

In the frame work of the simple dynamics expressed in equations (2.1, 2) and the analysis technique developed here, it is possible to make inferences on the wind stress acting on the ocean surface. Once the expansion coefficients P_α are determined from the objective analysis of the altimetric residuals, one can immediately calculate

$$\vec{F} = (\lambda \underline{I} - \underline{C})\ \vec{P} \tag{3.6}$$

from equation (2.16). The elements of the column vector $\vec{F}$ are essentially the projections of the wind stress curl on the various stream function modes as shown in equation (2.14). Let Ω be the stream function of the wind stress so that

$$\tau_x = -\frac{\partial \Omega}{\partial y},\ \tau_y = \frac{\partial \Omega}{\partial y}. \tag{3.7}$$

Then we can write from equation (2.14)

$$F_\alpha = -\frac{1}{H}\int \psi_\alpha\, \nabla^2\, \Omega\ dA \tag{3.8}$$

If Ω is now expressed as

$$\Omega = \sum_\alpha R_\alpha\, \psi_\alpha \tag{3.9}$$

and (3.9) is substituted into equation (3.8), the result is

$$R_\alpha = H\, F_\alpha$$

and (3.10)

$$\Omega = \sum_{\alpha} H F_{\alpha} \psi_{\alpha}$$

after using equation (2.8) and the orthogonality condition (2.11). This step determines the stream function for the wind stress Ω through (3.10). Therefore, it is now possible, in principle, to compute the rotational part of the wind stress both in magnitude and direction using altimetric residuals of sea surface topography and the analysis technique developed here. However, it should be noted that in the calculation of $\overline{F}$ and R_{α} through equations (3.6 and 10) the numerical values assigned to the depth H and friction coefficient enter explicitly. Since neither of these parameters are in the nature of universal constants, the inference on the magnitude of the stress would be doubtful since they directly influence R_{α} through (3.6 and 10). But the directionality of the wind stress should be more reliable since λ occurs only in the matrix in equation (3.6) that determines F_{α}.

Since an altimetric mission provides wind speed but not direction (Brown *et al,* 1981) the procedure advocated here raises the possibility of being able to assign directionality to the rotational part of the mean wind stress. Such a capability gives an opportunity to check the wind stresses measured from an altimeter and a scatterometer for consistency. Even though it is a reasonable assumption, it should be borne in mind that the present analysis procedure is based upon the premise that the large scale wind stress is nondivergent. In any case, since the wind speeds can be obtained directly from the altimetric measurements it is also possible to make an estimate of the depth H of a "wind driven ocean" using equations (3.7 and 10).

RESULTS FOR AN IDEAL BASIN CASE

In this preliminary study, the above analysis will be applied to an ocean basin of an ideal shape. The specific case considered is a rectangular ocean on a β-plane. The reason for considering a simple case like this is simply because the solution to this case is well known and the ability of the above objective analysis procedure using the characteristic functions in reproducing the known solution can be easily tested before attempting to apply the technique to more complicated cases of real ocean basins. In addition the problem can be solved by semi-analytic procedure as well as by purely numerical approach allowing the possibility to judge the effects of discretization errors. Consider a rectangular basin $O \leq X \leq L$ and $O \leq Y \leq B$. The solution to the characteristic value problem (2.8) is

$$\psi_{\alpha} = \frac{2}{\sqrt{BL\mu_{\alpha}}} \cdot \operatorname{Sin} \frac{m_{\alpha} \pi x}{L} \operatorname{Sin} \frac{n_{\alpha} \pi y}{B} \tag{4.1}$$

$$\mu_{\alpha} = \pi^2 \left(\frac{m_{\alpha}^2}{L^2} + \frac{n_{\alpha}^2}{B^2} \right)$$

m_{α} and n_{α} (integers)

The above solution for ψ_{α} takes into account the orthonormality condition (2.11). The basic stream function modes are simply gyres. The number of gyres inside the basin depends on the integer values of m_{α} and n_{α}. Figure 1 (top left and right panels), computed from (4.1) on a grid of $\Delta x = L/50$ and $\Delta y = B/25$ shows the patterns for two modes: $m_{\alpha} = 1 = n_{\alpha}$ and $m_{\alpha} = 2 = n_{\alpha}$. For natural basins the important starting point, namely the solution to (2.8), will have to be constructed using numerical methods. This was done by using a grid of $\Delta x = L/50$ and $\Delta y = B/30$ in solving for the characteristic values and functions resulting in 1421 interior points for ψ_{α}. The matrix of 1421×1421 was solved using a Lanczos procedure in which each Lanczos function at an iteration was orthogonalized with respect to all the preceding ones. The details of the general Lanczos procedure are not discussed here for the sake of brevity (see Platzman 1975 for details). Figure 1 (bottom panels) show the numerically calculated characteristic functions that correspond to the analytic ones shown in the top panels of Figure 1. A comparison of the analytical and numerical solutions shows an excellent ability of the numerical procedure to compute the necessary basis functions needed for the present analysis. Using (4.1) the elements of the matrix $\underline{C}$ are given by:

$$C_{\gamma\alpha} = \frac{4\beta}{L\sqrt{\mu_{\alpha}\,\mu_{\gamma}}} \frac{m_{\gamma}\, m_{\alpha}}{(m_{\gamma}^2 - m_{\alpha}^2)} \tag{4.2}$$

provided

$$m_{\alpha} - m_{\gamma} \text{ is odd and } n_{\alpha} = n_{\gamma}$$

The wind stress acting on the surface is taken to be

$$\tau_x = -\operatorname{Sin} \frac{\pi x}{L} \operatorname{Cos} \frac{\pi y}{B}$$

$$\tau_y = \frac{B}{L} \operatorname{Cos} \frac{\pi x}{L} \operatorname{Sin} \frac{\pi y}{B} \tag{4.3}$$

$$\Omega = \frac{B}{\pi} \operatorname{Sin} \frac{\pi x}{L} \operatorname{Sin} \frac{\pi y}{B}$$

This wind stress field is free of divergence and represents a simple anticyclonic gyre. Ω is the stream function associated with the above stress. The forcing elements F_{α} defined in (2.14) are given by:

$$F_{\alpha} = \frac{B\sqrt{BL\mu_{\alpha}}}{2\pi H} \text{ for } m_{\alpha} = n_{\alpha} = 1 \text{ only} \tag{4.4}$$

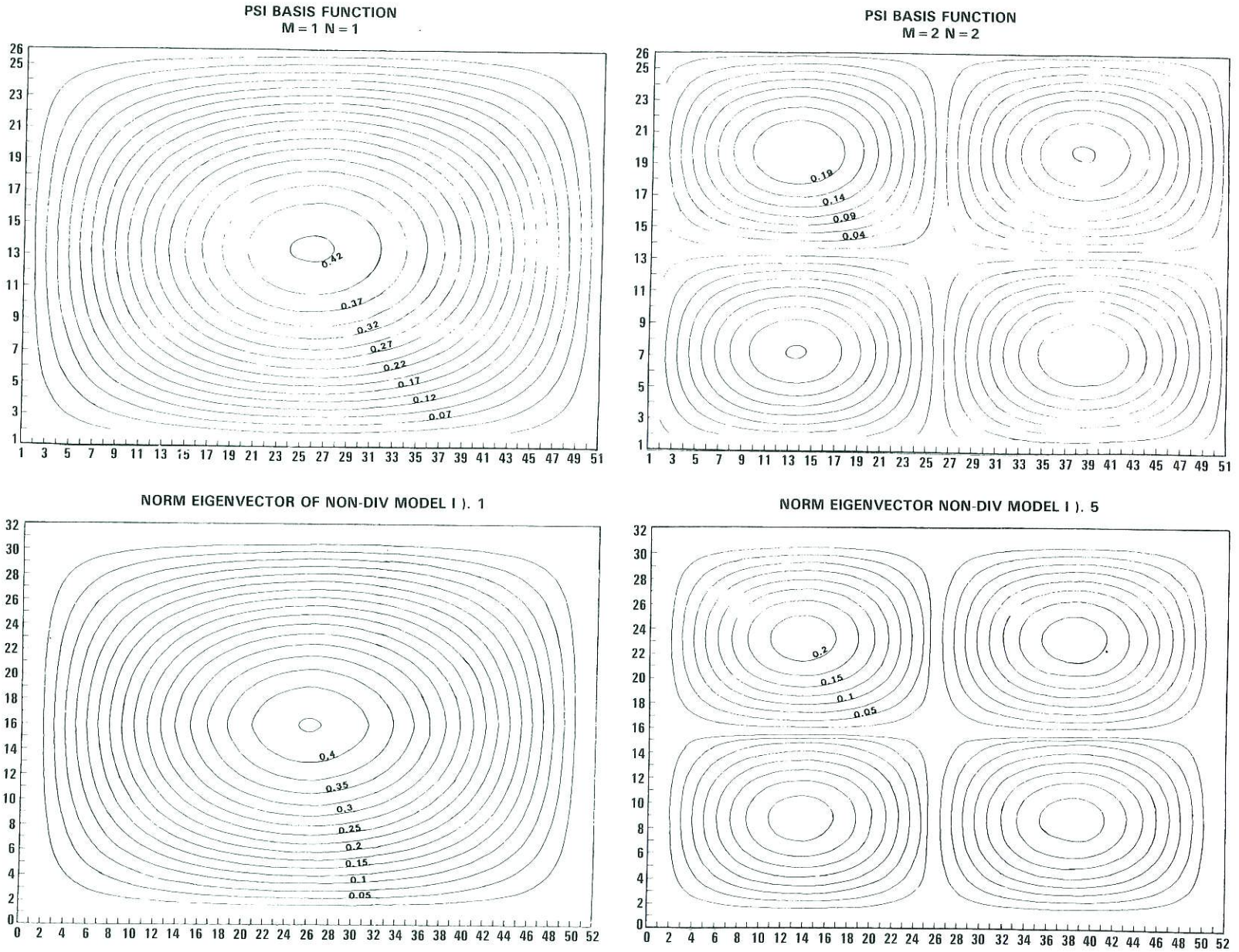

Figure 1: Pattern of the basis stream function modes corresponding to $m_\alpha = n_\alpha = 1$ (left panels) and $= 2$ (right panels). In each case the top panel corresponds to the analytic solution (Equation 4.1) and the bottom panel to the numerical solution from the Lanczos procedure. The units are nondimensional.

In view of the simple form of the assumed wind stress field, it has a non-trivial projection on only the stream function mode that corresponds to the integers $m_\alpha = 1 = n_\alpha$. The expansion coefficients P_α required in equation (2.10) to determine the stream function associated with steady circulation are obtained by solving equation (2.16). This can now be accomplished using the coefficients given in equations (4.2 and 4). The parameter values used in the numerical computations are:

$$\begin{aligned} L &= 10^9 \text{ cm.} \\ B &= 2\,\pi\,.10^8 \text{ cm.} \\ \beta &= 2.315\,.10^{-13}/\text{cm. sec} \\ g &= 981 \text{ cm/sec}^2 \\ \lambda &= 10^{-5}/\text{sec} \\ H &= 2.10^4 \text{ cm.} \end{aligned}$$

Several values of λ were tried. For $\lambda << 10^{-5}$, the inversion of the matrix in equation (2.16) does not converge well. For values of $\lambda >> 10^{-5}$, the flow field tends to be very damped. As a compromise, the value of $\lambda = 10^{-5}$ was used in the calculations reported here. As mentioned earlier, the exact values of λ and H are not definable but also, as previously noted, the basis functions for the height and stream fields used in the objective analysis are not affected by the choice of the numerical values of these two parameters. Consider now the problem defined by equations (2.18, 19) which give the characteristic functions for the height field. The solution for these functions is:

$$\zeta_\alpha = \frac{2}{g\sqrt{BL\mu_\alpha}}\left[f \operatorname{Sin}\frac{n_\alpha \pi y}{B} + \frac{\beta B_\alpha}{L_\alpha^2 + B_\alpha^2} \operatorname{Cos}\frac{n_\alpha \pi y}{B}\right] \operatorname{Sin}\frac{m_\alpha \pi x}{L} \tag{4.5}$$

where

$$L_\alpha \equiv m_\alpha \pi / L \text{ and } B_\alpha \equiv n_\alpha \pi / B.$$

Figure 2 (top panels) show two of these height field basis functions corresponding to $m_\alpha = 1 = n_\alpha$ and $m_\alpha = 2 = n_\alpha$. (Here f is simply taken as βy.) The number of gyres is again determined by the integer values of m_α and n_α. In the east-west direction, the number of gyres is the same as the integer value of m_α. If the integer value of n_α is i, there are i-1 closed gyres in the north-south direction and the southern most gyre exhibits the pattern of an open oval. When the numerically determined stream function modes are used to solve for the height field modes from (2.18, 19), the problem is reduced to inverting a matrix of 1519 × 1519 using the 51 × 31 grid. The matrix is very sparse and can be easily inverted using available computer subroutines. Figure 2 (bottom panels) shows the height field functions obtained numerically that correspond to the analytical ones in the top panels of Figure 2. Once again the agreement between the analytic functions and the numerical ones is excellent.

Substitution of the P_α's obtained from the solution of equation (2.16) into (2.10) yields the stream function of the circulation driven by the wind field given in equation (4.3). Figure 3 (bottom) shows the circulation field synthesized using 60 characteristic modes. In view of the conditions stated in (4.2, 4) the ordering of m_α and n_α with respect to the scalar index α was prescribed as

$$m_\alpha = \alpha \text{ for } \alpha = 1, 2, \ldots . N$$

$$n_\alpha = 1 \text{ for all } \alpha$$

where N is the maximum number of modes taken into consideration.* The figure shows the classical westward intensification of the circulation as shown by Stommel (1948). The maximum value of the transport occurs approximately at a distance of one fifth of the length of the basin from the western boundary. The precise location of the maximum is governed by the choice of λ. For example, when $\lambda = 0.4 \times 10^{-5}$, the maximum occurs at a distance of about 1/10th of L from the western boundary. The vorticity equation (2.4) can be solved exactly for the forcing function given by (4.3). The solution in terms of the stream function is:

$$\begin{aligned} \psi = K \Bigg\{ & \frac{\pi\lambda}{\beta L}\left(\frac{L^2}{B^2} + 1\right) \operatorname{Sin}\frac{\pi x}{L} + \operatorname{Cos}\frac{\pi x}{L} \\ & + \frac{\left[1 + e^{-\left(\frac{\beta}{2\lambda} + \theta\right)L}\right]}{e^{-\left(\frac{\beta}{2\lambda} - \theta\right)L} - e^{-\left(\frac{\beta}{2\lambda} + \theta\right)L}} \cdot e^{-\left(\frac{\beta}{2\lambda} - \theta\right)x} \\ & - \frac{\left[1 + e^{-\left(\frac{\beta}{2\lambda} + \theta\right)L}\right]}{e^{-\left(\frac{\beta}{2\lambda} - \theta\right)L} - e^{-\left(\frac{\beta}{2\lambda} + \theta\right)L}} \cdot e^{-\left(\frac{\beta}{2\lambda} + \theta\right)x} \Bigg\} \operatorname{Sin}\frac{\pi y}{B} \end{aligned} \tag{4.6}$$

$$K \equiv \frac{B^2 + L^2}{\lambda\pi + B} \cdot \left(\frac{1}{\left(\frac{L^2}{B^2} + 1\right)^2 + \frac{\beta^2 L^2}{\pi^2\lambda^2}}\right) \frac{\beta L}{\lambda\pi}$$

*An additional 50 modes with randomly assigned integer values to m_α and n_α were included in the computation to see their impact on the numerical process of calculating P_α. The calculations were completely unaffected by the presence of these additional modes and the P_α values for all of them were calculated to be zero.

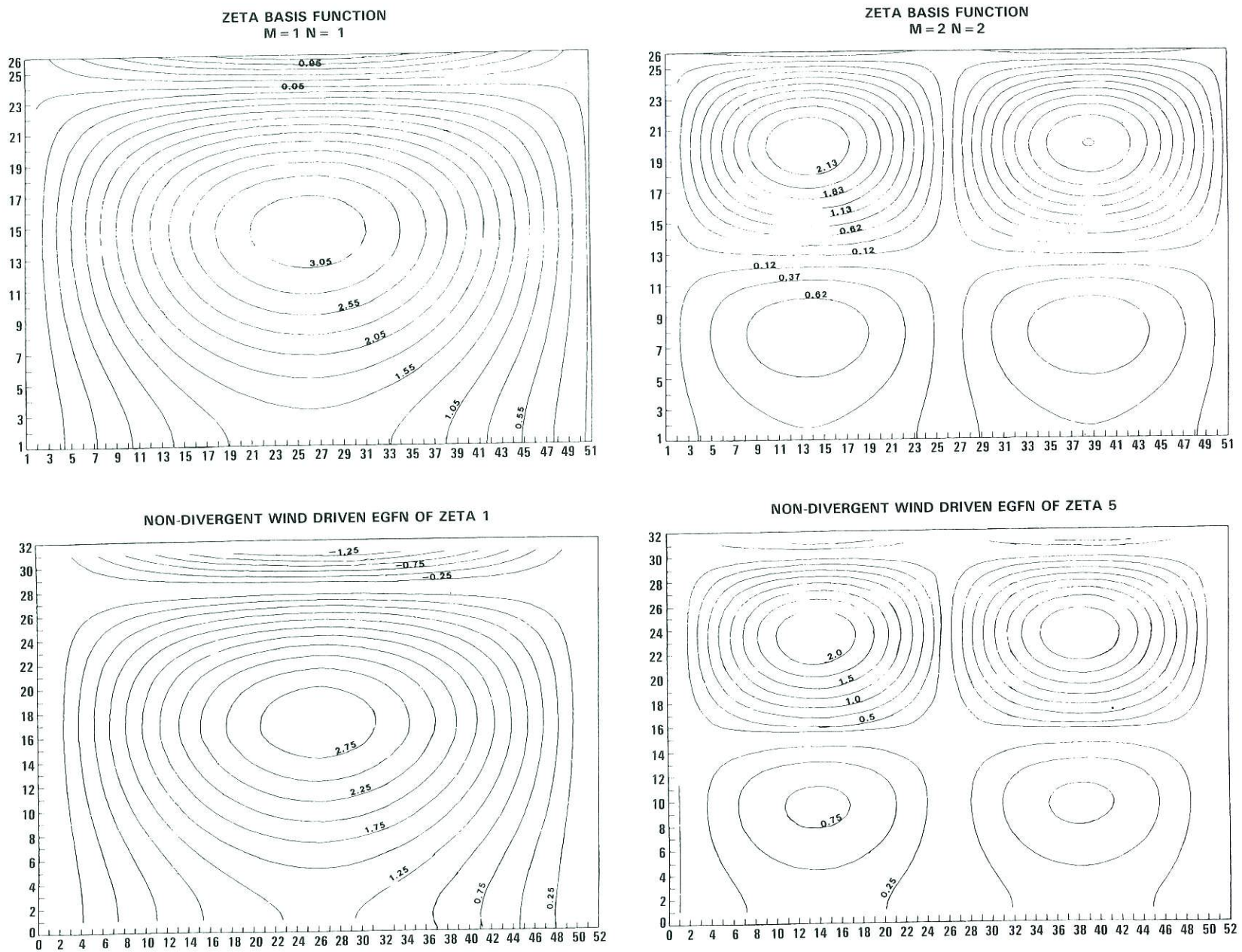

Figure 2: Same as in Figure 1 but the patterns are for the height field functions. The units are in sec/cm.

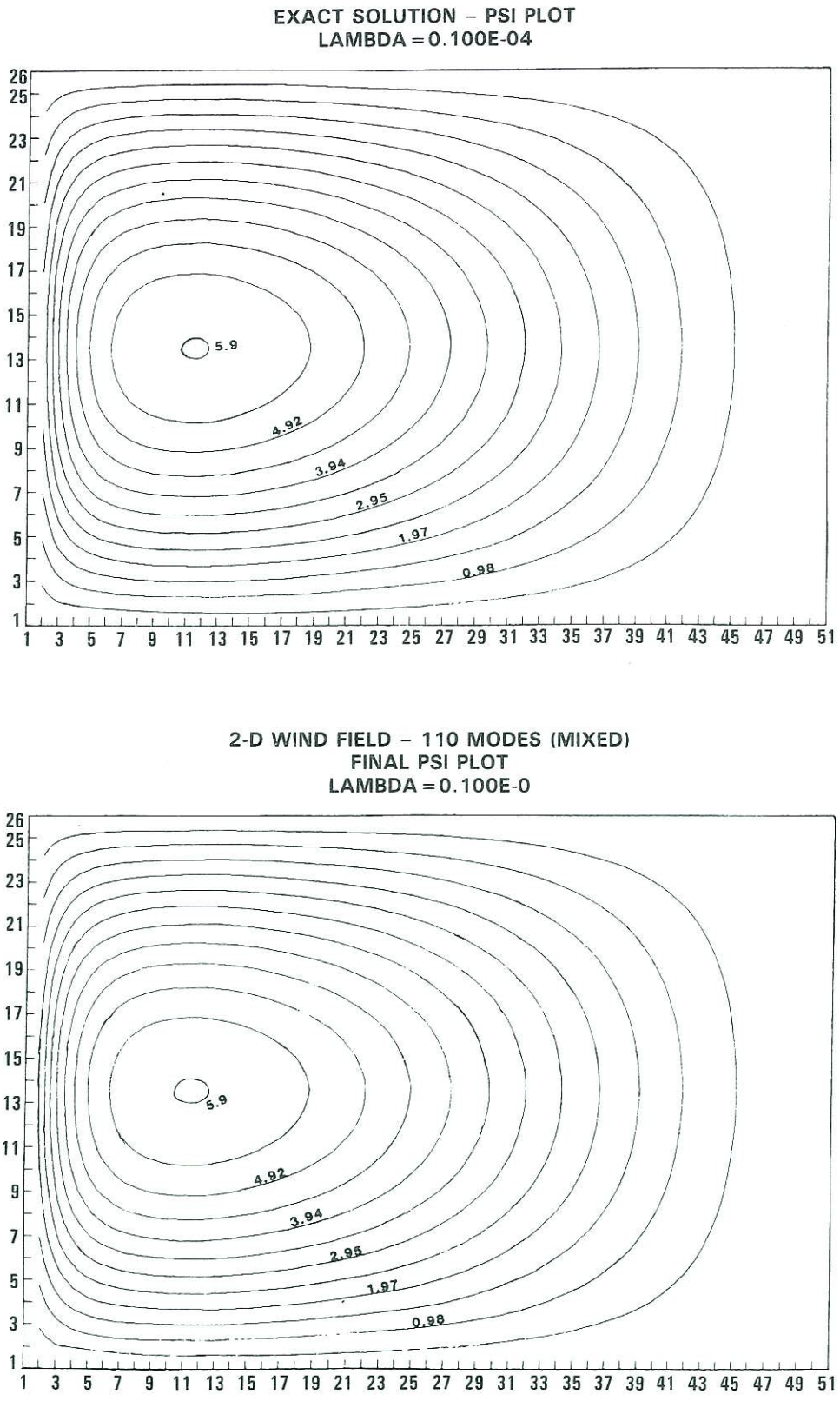

Figure 3: Stream function pattern for the wind driven circulation. Top panel corresponds to the exact solution and the bottom panel to the spectral solution. The units are in 10^8 cm^2/sec.

$$\theta \equiv \left(\frac{\pi^2}{B^2} + \frac{\beta^2}{4\lambda^2}\right)^{1/2}$$

Figure 3 (top) shows a plot of the above exact solution to the problem. Comparison of top and bottom panels of Figure 3 shows an excellent agreement between the spectral solution and the exact solution.

The sea surface topography associated with the circulation can now be computed using the expansion coefficients P_α in equation (2.17) and the height field basis functions given in (4.5). Figure 4 illustrates this topography which also exhibits a highly asymmetric pattern. Basically it consists of a high pressure pattern over most of the basin with the maximum occurring approximately at a distance of L/5 from the western boundary and slightly greater than B/2 from the southern boundary of the basin. Contours of surface topography intersect the equator as shown in the figure. The solution in Figure 4 can be viewed as the sea surface topography obtained from a perfect altimetric mission—namely, one without any contamination from the various sources of error mentioned earlier. Application of simple geostrophic considerations to compute the flow from the topography in Figure 4 obviously is going to provide a circulation pattern that will not resemble the actual one shown in Figure 3 over most of the basin and particularly along the southern boundary where f=0.

In performing the objective analysis, we consider the data field shown in Figure 4 as the "true" data field. If one suppresses a certain amount of data and performs the objective analysis on the remainder to reconstruct the height field, the "true" solution would serve as a basis to estimate the accuracy or fidelity of the analysis procedure. If the basin considered were a real ocean basin, the elimination of the residuals would take into account the errors expected in the retrievals from the sources mentioned earlier over various parts of the ocean basin. Since the basin under consideration here is a simple idealized one, we have suppressed the data on a purely random basis and performed objective analysis on the remaining data without introducing any errors in the data. The height field shown in Figure 4 was calculated on a grid of 51×26 which gives a total number of 1274 data points because of the boundary condition (2.19). The analysis was performed on randomly selected sets of 300, 600, and 900 error free data points using in each case 30 and 40 modes. The results are summarized in Tables 1 and 2.

An examination of Tables 1 and 2 shows clearly that the objective analysis has done a remarkable job in recovering the "true" solution with as few as approximately one quarter of the total data points available using 30 modes. Figure 5 shows the surface topography (top panel) and the stream function field (bottom panel) recovered from the objective analysis using 30 modes and 300 randomly selected data points.

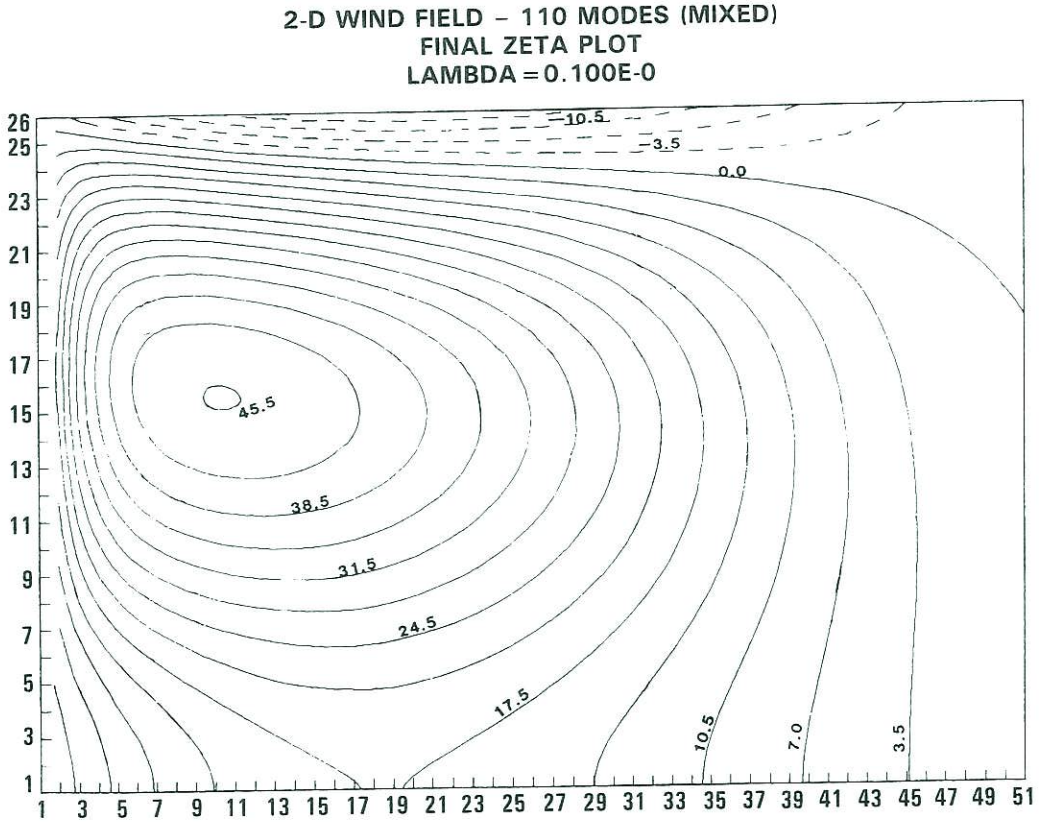

Figure 4: Sea surface topography pattern (in cms.) associated with the circulation shown in Figure 3.

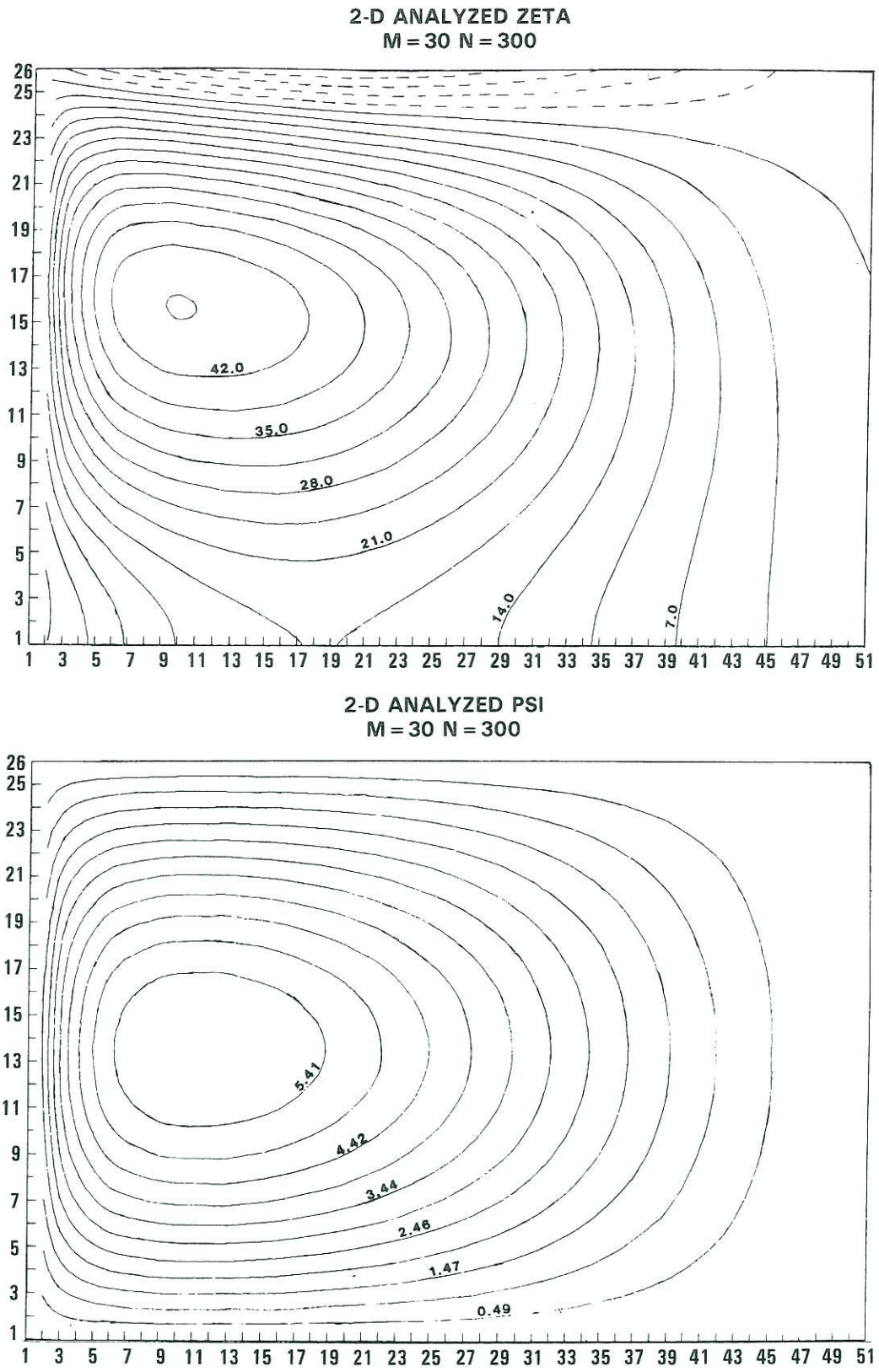

Figure 5: Sea surface topography (top) and stream line (bottom) patterns obtained from objective analysis of error free data from 300 randomly selected data points using 30 functions.

Table 1: Results of objective analysis for ζ (in cm) using error free data.

No. of modes	No. of points	RMS difference for Zeta at data points	RMS difference for Zeta over the basin	Maximum and minimum value for Zeta from analysis	theory
30	300	0.0027	0.0017	45.54,-17.54:	45.53, 17.54
	600	0.0024	0.0017	45.53,-17.54	
	900	0.0019	0.0017	45.53,-17.54	
40	300	0.0007	0.0004	45.55,-17.54	
	600	0.0005	0.0004	45.55,-17.54	
	900	0.0004	0.0004	45.55,-17.54	

Table 2: Results for ψ (in cm^2/sec)

No. of modes	No. of points	RMS difference for psi at data points ($\times 10^5$)	RMS difference for psi over the basin ($\times 10^5$)	Maximum * value for psi from analysis ($\times 10^9$)	theory
30	300	0.345	0.215	0.5899	0.5903
	600	0.309	0.213	0.5903	
	900	0.236	0.213	0.5903	
40	300	0.088	0.049	0.5901	
	600	0.066	0.048	0.5902	
	900	0.053	0.047	0.5902	

*Minimum value for ψ is zero on the boundary

Comparison with Figures (4 and bottom panel of 3) shows the closeness of the analyzed patterns to the theoretical ones. Figure 6 shows the stream function Ω of the wind stress field obtained through the objective analysis procedure (top panel) and the actual one given in (4.3) (bottom panel) that was used in the theoretical solution. Once again it is seen, at least in the simple case considered here, that the analysis procedure yields an unambiguous recovery of the rotational part of the driving force. As cautioned earlier, the magnitude of the wind stress depends on the numerical values assigned to λ and H.

The effect of assuming a λ different from the one that has been used in generating the ''true'' solution on the retrieval of the *wind stress stream function* from the objective analysis is shown in Figure 7. In the theoretical calculation, λ was taken to be 10^{-5}. The λ values used in Figure 7 are 0.5×10^{-5} (top) and 10^{-6} (bottom). It is seen from these figures that the stream function pattern of the wind stress is still reproduced fairly well over most of the basin. It is only in the westernmost part of the basin, where the circulation is strongest and hence is a region of largest friction, do the actual and retrieved wind field directions differ. The magnitude, of course, has also changed. These different values of λ, however, have absolutely no effect on the analysis for the surface topography and the stream function of the flow field presented in Figure 5 since the calculation of P_c from the data does not involve the use of λ or H.

In order to consider the effect of errors in the data on the objective analysis procedure, an error of $\pm$ 10% was introduced randomly into the 300 data points. The result of analysis using 30 height field basis functions is shown in Figure 8 for the height field (top left), flow field (top right) and the wind stress stream function with $\lambda = 0.5 \times 10^{-5}$ (bottom left) and 10^{-6} (bottom right) instead of 10^{-5} that was used in generating the theoretical data base. The resulting fields were subjected to a smoothing according to:

$$\overline{C}_{ij} = 0.8\, C_{ij} + 0.05\, [C_{i+1,j} + C_{i-1,j} + C_{i,j+1} + C_{i,j-1}]$$

As expected the contours exhibit some wiggles instead of being smooth as with the error free data. The rms differences and the maximum and minimum values resulting from the analysis of the data with noise are shown in Table 3 (note that these numbers are independent of the λ value):

Table 3: Results from data with introduction of errors.

	RMS difference		Maximum	Minimum
	at data points	whole basin	of the dependent variable	
ζ (cm)	0.025	0.012	45.88	−17.55
ψ (cm^2/sec)	3.2 (10^5)	1.5 (10^5)	5.93 (10^8)	0

The differences are still quite small and the maximum and minimum values of the height field and the stream function of the flow field are determined very well. The patterns of these fields still exhibit a close resemblance to the theoretical solutions. Once again, the direction of the wind stress resulting from the analysis agrees with the actual one over a large part of the basin with the exception of the westernmost region as noted previously.

Finally it should also be noted that as far as the objective analysis of the height field and recovery of the flow field are concerned, there is no implied assumption that the ocean dynamics are steady. The height field basis functions are related to those of the flow field through a purely diagnostic equation (2.18) because both the ocean circulation and the wind stress are assumed to be non-divergent. The expansions (2.10 and 17) for the forced stream function and the surface topography are still valid even if the circulation is non-steady. In the above examples, we have chosen to present the results of objective analysis for a steady-state situation only for convenience.

CONCLUSION

Using a simple dynamical model of wind driven ocean circulation with linear bottom friction, an analytical basis was developed to objectively analyze the sea surface topography derived from altimetric residuals and, in the process, deduce the total flow instead of just the geostrophic component of the circulation. The primary assumptions of the theory are that both the ocean circulation and the surface wind stress are free of divergence. The method depends on constructing a set of basis functions for the stream function of the flow field and a set of basis functions for the height field. The basis functions for the flow field are solutions of a homogeneous elliptic equation. The analysis shows that the appropriate set of basis functions for the height field are solutions of an inhomogeneous balance equation. When the functions are chosen in this particular way, the theory shows that in the spectral representatation of an arbitrary flow field and the associated height field in terms of these basis functions, the expansion coefficients for both fields are the same. Hence, when the sea surface topography is prescribed from altimetric measurements, after eliminating data in regions of serious uncertainty in the retrievals due to various sources of error, the height field functions can be used to objectively analyze the remaining data through least squares procedures and determine the expansion coefficients. The basis stream function modes then yield the total stream function of the flow associated with the topography.

Even though the dynamical basis adopted here is a simple wind driven circulation model of Stommel, it is certainly more complicated than the simple application of geostrophic dynamics in extracting ocean circulation information from altimetry. In particular, the method described here does not suffer from the fatal breakdown in the equatorial regions like the geostrophic dynamics do. Considering that the tropical ocean circulation is one of the most important ingredients in the air-sea interactions on a climatic scale, the method outlined here allows the possibility of extracting the oceanographic signal in the tropics in a more reliable manner. Moreover, since the basis functions can be constructed for an ocean basin taking into account the geometric irregularities and the necessary boundary conditions, they would constitute a better set of functions in analyzing the data than any analytical functions that are oblivious of the basin geometry. An additional feature of the analysis is that it allows the possibility of assigning a direction to the surface wind stress that is responsible for maintaining the given surface topography. Even though this study considered only linear wind driven ocean dynamics, the method can be extended to consider nonlinear aspects if necessary.

The numerical modelling of ocean circulation has not yet matured to the stage of using real data to initialize the models and to consider problems of data assimilation like the atmospheric models do; sparsity of oceanographic data being at least one of the reasons. With the advent of various ocean related satellite missions and *in-situ* data collection programs under planning in conjunction with the World Climate Research Program, substantial amounts of oceanographic data will soon be available. Some of the considerations presented in this study would become useful in initializing and balancing different data fields for future numerical ocean modeling efforts.

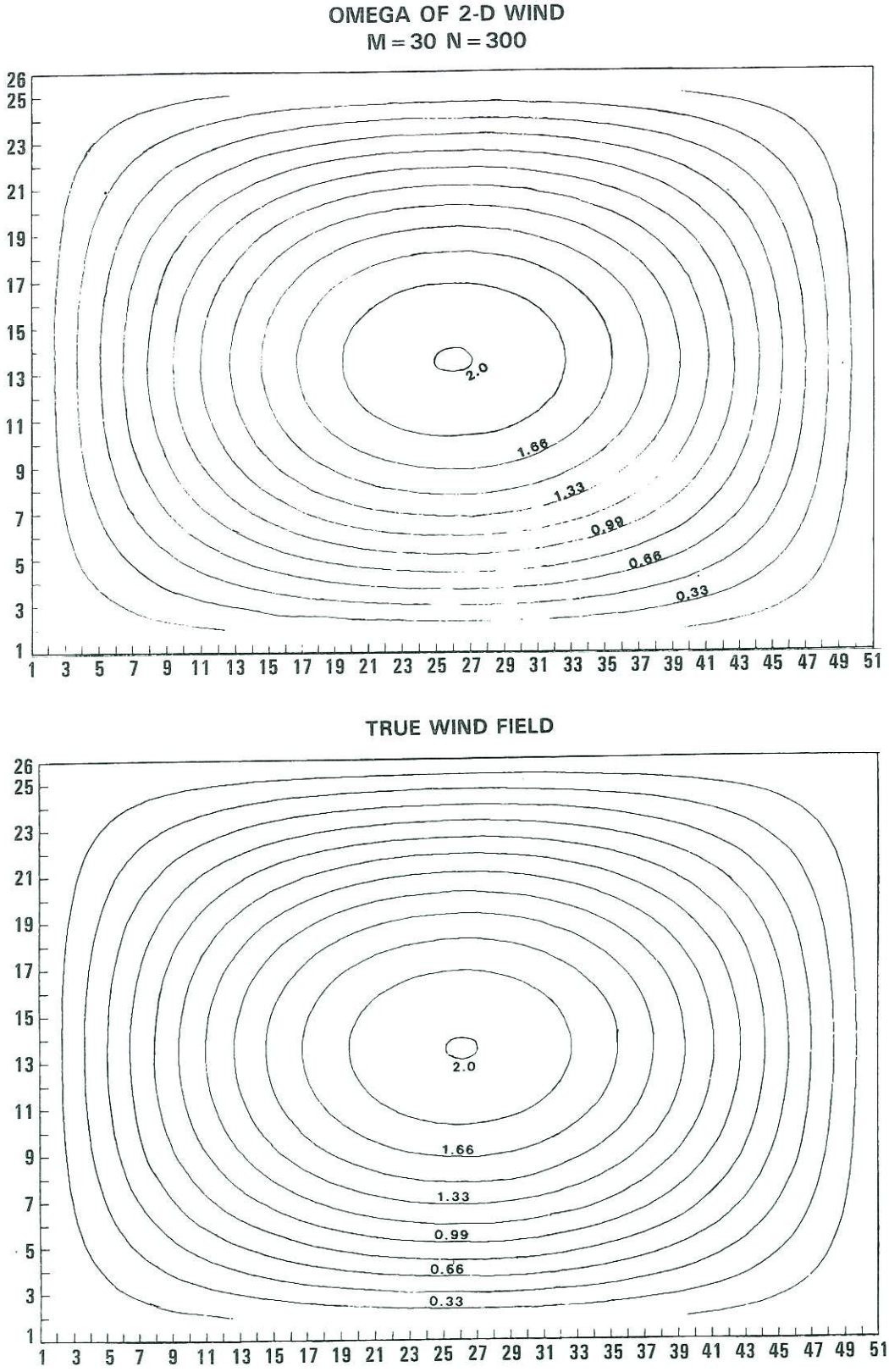

Figure 6: Stream function of the wind stress field in units of 10^9 cm^3/sec^2. Top panel is the field obtained from the objective analysis procedure using $\lambda = 10^{-5}$. The bottom panel is the actual wind field that was prescribed in the theoretical calculations.

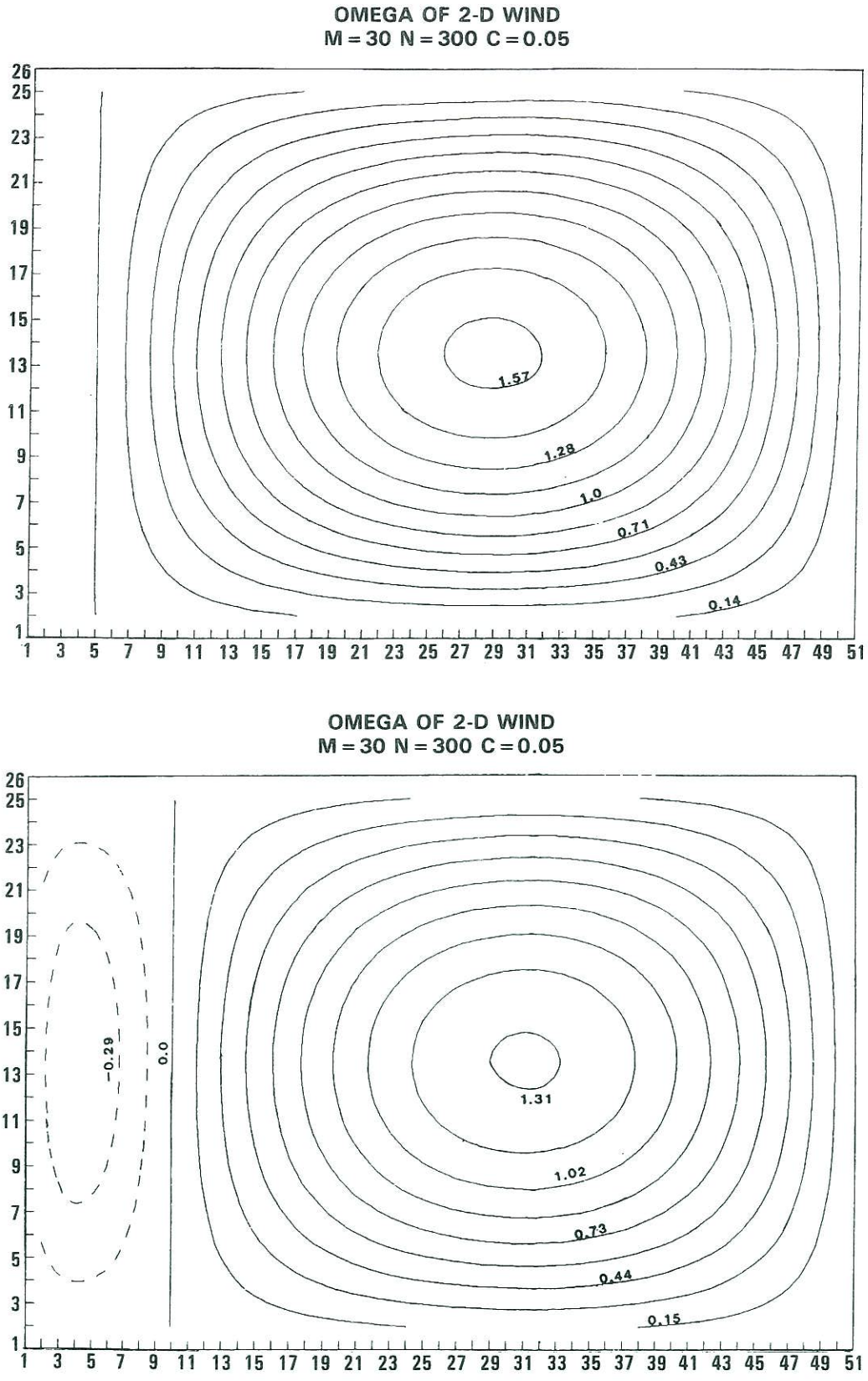

Figure 7: Stream function of the wind stress from objective analysis using different values of $\lambda = 0.5 \times 10^{-5}$ (top) and 10^{-6} (bottom).

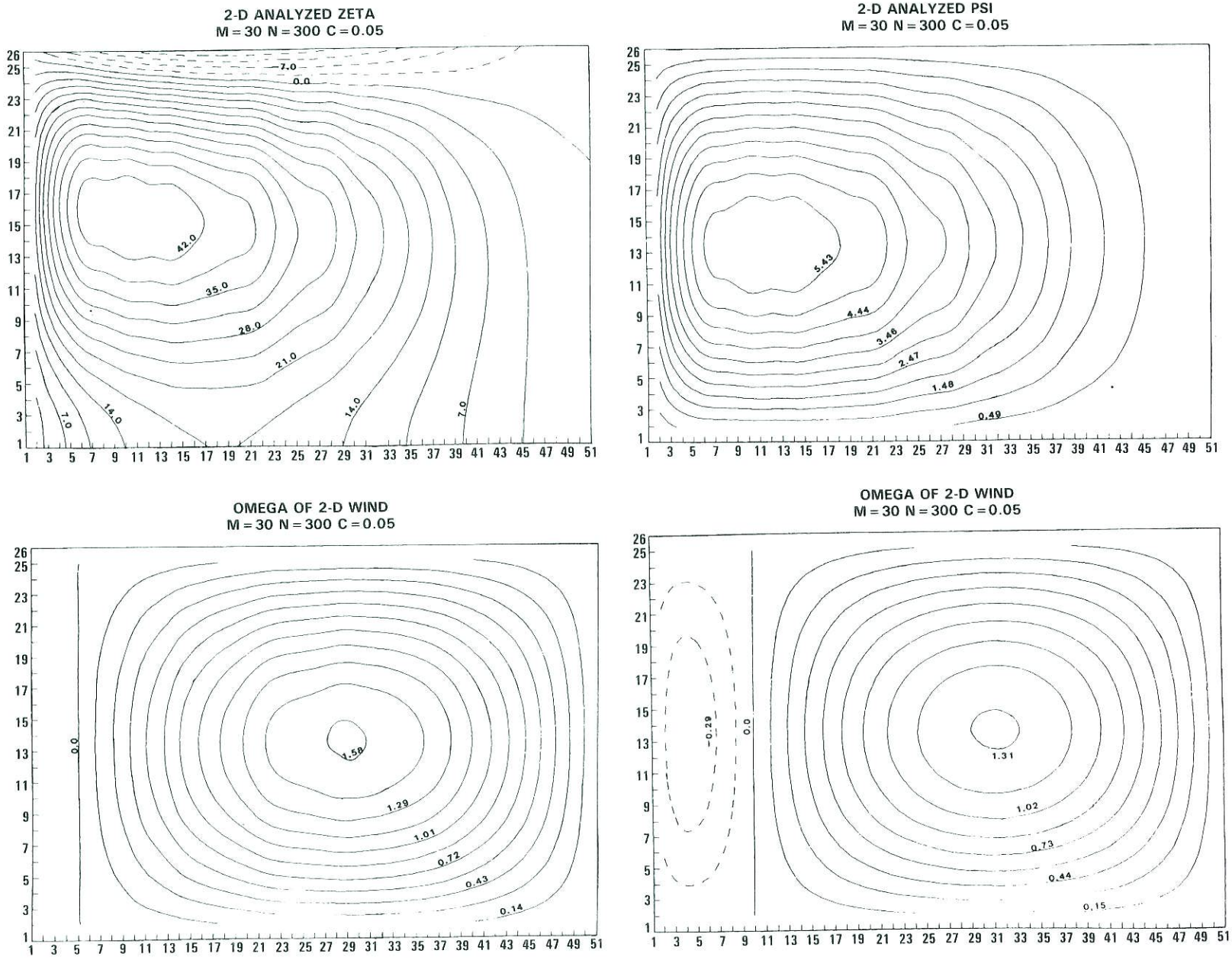

Figure 8: Results of objective analysis of surface topography data taken at 300 random points with $\pm$ 10% errors introduced randomly: height field (top left), stream function of the circulation (top right). Stream function of the wind field (with $\lambda = 0.5 \times 10^{-5}$ in the bottom left and 10^{-6} in the bottom right panels).

The theory was tested in this preliminary study on an ideal rectangular basin located north of the equator on a β-plane. First a theoretical solution for the stream function of the flow and the resulting surface topography for a given wind stress were obtained. Using the theoretical field of the topography as a "true" data field, a randomly selected set of data points were subjected to the objective analysis using the height field basis modes through a least squares technique. The expansion coefficients thus determined and the corresponding basis functions were then used to reconstruct the height field and the flow field over the whole basin. Comparison with the "true" data fields shows that the objective analysis procedure does an exceedingly good job in recovering the "true" solution with as few as a quarter of the total available data in this ideal basin case. It was also shown that the effect of introducing random error of $\pm$ 10% at all data points does not seriously affect the results. As pointed out in Section 3, the calculation of the direction of the wind stress depends on the value assumed for the linear bottom friction coefficient. The calulations presented show that the direction of the wind stress is given with reasonable accuracy over most of the basin even when the bottom friction coefficient was varied over an order of magnitude.

The technique discussed here is fully adaptable to complete numerical treatment and hence is applicable to real ocean basins. Calculations are in progress on the Atlantic-Indian Ocean system with the effect of topography also taken into account and will be reported shortly.

Acknowledgements: The work reported here was supported by the Oceanic Processes Branch of NASA. We are grateful for a critical review of the manuscript by Norman Phillips.

REFERENCES

Brown, G.S., H.R Stanley, and N.A. Roy, 1981: Wind speed measurement capability of spaceborne radar altimeters. IEEE J. Ocean Engineering, OE 6, 59-63.

Platzman, G.W., 1975: Normal modes of the Atlantic and Indian Oceans. J. Phys. Oceanog., 5, 201-221.

Rao, D.B., 1966: Free gravitational oscillations in rotating rectangular basins. J. Fluid Mech., 25, 523-555.

Rao, D.B., 1974: Transient response of shallow enclosed basins using the method of normal modes. Scientific Series No. 38, Inland Waters Directorate, Environment Canada, 38 pp.

Rao, D.B., and D.J. Schwab, 1976: Two dimensional normal modes in arbitrary enclosed basins on a rotating earth: Application to Lakes Ontario and Superior. Phil. Trans. Royal Soc. London, Ser. A, 281, 63-96.

Rao, D.B., and D.J. Schwab, 1981: A method of objective analysis for currents in a lake with application to Lake Ontario. J. Phys. Oceanog., 11, 739-750.

Reid, R.O., 1958: Effect of Coriolis force on edge waves. (1) Investigation of normal modes. J. Mar. Res., 16, 109-141.

Report of the TOPEX Scientific Working Group, 1981: Satellite altimetric measurements of the ocean. Jet Propulsion Laboratory Publication, March 1981, 78 pp.

Sanchez, B.V., D.B. Rao, and P.G. Wolfson, 1985: Objective analysis for tides in a closed basin. Mar. Geod., 9, 71-91.

Stommel, H., 1948: The westward intensification of wind-driven ocean currents. Trans. Amer. Geoph. Union, 29, 202-206.

Tai, C.K., 1983: On determining the large-scale ocean circulation from satellite altimetry. J. Geophy. Res., 88, 9553-9565.

Tai, C.K., and C. Wunsch, 1983: Absolute measurements by satellite altimetry of dynamic topography of the Pacific Ocean. Nature, 301, 408-410.

Wunsch, Carl, and E.M. Gaposchkin, 1980: On using satellite altimetry to determine the general circulation of the oceans with application to geoid improvement. Rev. of Geophysics and Space Physics, 18, 725-745.

BIBLIOGRAPHIC DATA SHEET

1. Report No. NASA TM-87799	2. Government Accession No.	3. Recipient's Catalog No.
4. Title and Subtitle A METHOD OF CALCULATING THE TOTAL FLOW FROM A GIVEN SEA SURFACE TOPOGRAPHY		5. Report Date April 1987 6. Performing Organization Code 621
7. Author(s) Desiraju B. Rao*, Stephen D. Steenrod**, and Braulio V. Sanchez ***		8. Performing Organization Report No. 87B0128
9. Performing Organization Name and Address NASA/Goddard Space Flight Center Code 621/Geodynamics Branch Greenbelt, MD 20771		10. Work Unit No. 11. Contract or Grant No. 13. Type of Report and Period Covered Technical Memorandum
12. Sponsoring Agency Name and Address National Aeronautics and Space Administration Washington, D.C. 20546		14. Sponsoring Agency Code

15. Supplementary Notes

*National Meteorological Center, Washington, DC
**Applied Research Corporation, Landover, MD
***Goddard Space Flight Center Greenbelt, MD

16. Abstract

Using a simple dynamical model of a wind-driven ocean circulation of the Stommel type, an analytical basis was developed to objectively analyze the sea surface height residuals from an altimeter and, in the process, to determine the total flow instead of just the near surface geostrophic component associated with the given sea surface topography. The method is based upon first deriving the solution to the forced problem for a given wind stress required to develop a hypothetical "true or perfect" data field and to establishing the basis for the objective analysis. The stream function and the surface height field for the forced problem are developed in terms of certain characteristic functions with the *same expansion coefficients* for both fields. These characteristic functions are simply the solutions for a homogeneous elliptic equation for the stream function and the solutions of an inhomogeneous "balance" equation for the height field. For the objective analysis, using a sample of randomly selected height values from the "true" data field, the height field characteristic functions are used to fit the given topography in a least squares sense. The resulting expansion coefficients then permit the synthesis of the total flow field via the stream function characteristic modes and the solution is perfectly well behaved even along the equator. The method of solution is easily adaptable to realistic ocean basis by straight forward numerical methods. In this paper, the analytical basis of the theory and the results for an ideal rectangular basin on a beta plane are described.

17. Key Words (Selected by Author(s))	18. Distribution Statement
Sea Surface Topography, Wind-Driven Ocean Circulation, Stream Function, Objective Analysis, Satellite Altimetry	Unlimited — Unclassified Subject Category 48

19. Security Classif. (of this report)	20. Security Classif. (of this page)	21. No. of Pages	22. Price*
UNCLASSIFIED	UNCLASSIFIED	24	A02

*For sale by the National Technical Information Service, Springfield, Virginia 22161

NASA-Langley, 1987

National Aeronautics and
Space Administration
Code NIT-4

Washington, D.C.
20546-0001